An efficient approach to separate CO_2 using supersonic flows for carbon capture and storage

Chuang Wen[1], Nikolas Karvounis[1], Jens Honore Walther[1, 2], Yuying Yan[3], Yuqing Feng[4], Yan Yang[1, *]

[1]Department of Mechanical Engineering, Technical University of Denmark, Nils Koppels Allé, 2800 Kgs. Lyngby, Denmark

[2]Computational Science and Engineering Laboratory, ETH Zürich, Clausiusstrasse 33, CH-8092 Zürich, Switzerland

[3]Faculty of Engineering, University of Nottingham, University Park, Nottingham NG7 2RD, UK

[4]CSIRO Mineral Resources, Bayview Avenue, Clayton VIC 3168, Australia

*Corresponding author: Yan Yang, Email: yyang@mek.dtu.dk

Abstract: The mitigation of CO_2 emissions is an effective measure to solve the climate change issue. In the present study, we propose an alternative approach for CO_2 capture by employing supersonic flows. For this purpose, we first develop a computational fluid dynamics (CFD) model to predict the CO_2 condensing flow in a supersonic nozzle. Adding two transport equations to describe the liquid fraction and droplet number, the detailed numerical model can describe the heat and mass transfer characteristics during the CO_2 phase change process under the supersonic expansion conditions. A comparative study is performed to evaluate the effect of CO_2 condensation using the condensation model and dry gas assumption. The results show that the developed CFD model predicts accurately the distribution of the static temperature contrary to the dry

gas assumption. Furthermore, the condensing flow model predicts a CO_2 liquid fraction up to 18.6% of the total mass, which leads to the release of the latent heat to the vapour phase. The investigation performed in this study suggests that the CO_2 condensation in supersonic flows provides an efficient and eco-friendly way to mitigate the CO_2 emissions to the environment.

Keywords: CO_2 separation, carbon capture and storage, supersonic flow, CO_2 emission

1 Introduction

Carbon capture and storage (CCS) has been proposed as a potential way to mitigate greenhouse gas emissions, such as carbon dioxide (CO_2) [1]. This can lead to a cleaner utilization of fossil energy [2], which has been recognised as one of the most promising measures to improve the sustainable development of the coal, oil and gas industries with regards to the CO_2 emission [3]. One of the promising applications is to use the captured CO_2 for the enhanced oil recovery and carbon storage in shale oil reservoirs [4]. Kim et al. [5] evaluated CO_2 injection in shale gas reservoirs considering the influences of the multi-component transport and geomechanical effects. Singh [6] evaluated the influence of CO_2 injection schemes on the reservoir pressure and saturation, and the results showed that the cyclic injection scheme is a better choice to store CO_2 in storage reservoirs. Zhang et al. [7] assessed the potential of CO_2 injection for the geological storage in geothermal reservoirs of China, and they presented three types of geothermal reservoirs suitable for CO_2 injection.

Currently, CO_2 can be removed using the following conventional techniques: absorption [8], adsorption [9], cryogenics [10] and membrane [11], which may have

some drawbacks, such as the relatively large facilities, a considerable investment, complex mechanical work, and the possibility of having a negative impact on the environment [12]. In addition, nanofluids have been used to enhance the CO_2 absorption for decades, including SiO_2 [13], Fe_3O_4 [14], Al_2O_3 [15] nanoparticles. The enhancement mechanisms of nanofluids can be explained by the grazing effect and the hydrodynamic effect in the gas-liquid boundary layer and inhibition of bubble coalescence. The detailed information about this novel approach can be found in a state-of-the-art review by Zhang et al. [16].

The supersonic separation, a revolutionary technique, has been introduced to remove water vapour from natural gas, which overcomes some of the disadvantages of conventional separation technologies [17]. The supersonic separation technology also provides a potential for CO_2 removal from natural gas contributing to CCS [18]. The condensable gas components are condensed to the liquid phase due to the extremely non-equilibrium state in supersonic flows [19]. The condensed liquids are then removed from the gas-liquid mixture on account of the high centrifugal force generated by swirling devices inserted into the flow channel [20]. As a static device, the supersonic separator has no rotating parts, enabling high reliability and availability. Furthermore, during these processes, the supersonic separation technology presents an environmental-friendly approach since it does not need any chemicals for CO_2 separation and also does not produce any pollution to the environments [21]. Therefore, the CO_2 supersonic separation is proposed as an alternative way to mitigate the CO_2 emissions to the environments from fossil power generation.

Most of the numerical studies on the supersonic separation in recent years are focused on the single-phase flow or particle flows without considering the condensation phenomenon. Secchi et al. [22] employed a 1D model and NIST REFPROP thermodynamics properties for the preliminary design of a supersonic separator involving the flow acceleration in a Laval nozzle and the swirling effects. Bian et al. [23] performed the structure optimization of the supersonic separator by using the assumption of the single-phase flow. Based on the assumption of the single-phase flow, Wang et al. optimized the geometrical parameters of the supersonic separator, such as the blade angle [24], discharge chamber [25] and reflow channel [26]. Niknam et al. [27] performed the numerical simulation on the flow behaviour inside a supersonic separator, including the detailed distribution of the static pressure, temperature and Mach number. Liu and Liu [28] numerically investigated the detailed distribution of the flow field inside the supersonic separator and analysed the effect of the static pressure in the shock wave position with the assumptions of single-phase flow and ideal gas model. Jiang et al. [29] employed the discrete particle method to predict the particle trajectories inside a supersonic separator based on the assumed particle size instead of the real condensed droplet size.

A few numerical studies have considered the condensing flow of water vapour in supersonic separators. Ma et al. [30] established a two-fluid flow model to investigate the spontaneous condensation of water vapour. Ma et al. [31] also studied the effect of the location where the external particles were added on the droplet condensation by using the heterogeneous nucleation theory, and proposed that it is reasonable to add

external nuclei to increase the size of the condensed droplets. Schooshtari et al. [32] developed a new theoretical approach based on the mass transfer rates to calculate the liquid droplet growth in supersonic conditions for binary mixtures, and also analysed the condensing flow of the multi-component gas mixtures with the nucleation theory [33]. Castier [34] carried out numerical simulations of natural gas flow within a Laval nozzle both considering both single-phase flow and phase equilibrium processes. Shooshtari and Shahsavand [35] developed the heterogeneous condensation model to optimize the supersonic separator for the removal of water vapour.

In the present study, we propose and evaluate the potential of the supersonic separation technique for CO_2 removal, which is still not comprehensively understood in the aforementioned studies. A computational fluid dynamics (CFD) model is developed to predict the non-equilibrium condensation phenomenon of CO_2 in supersonic flows. The developed CFD model is subsequently validated and verified against experimental data including the static pressure and droplet radius inside a high-pressure nozzle. The developed condensing flow model is further compared to the conventional dry gas assumption without considering the phase change to demonstrate the significant effect of the condensation process on the CO_2 supersonic separation. The condensation parameters of CO_2 under the supersonic non-equilibrium state is described in detailed including the nucleation rate, a liquid fraction and droplet radius.

2 Mathematical modelling

The nucleation and condensation of condensable gases are overwhelmingly complicated due to the non-equilibrium state in supersonic flows. For the mathematical

modelling of this kind of flow behaviour, the following assumptions are used in this study: a) external particles are neglected since the focus is on the spontaneous condensation phenomenon [36], b) the effect of gravitational forces is negligible in numerical simulations [37], c) the tiny condensed droplets follow the vapour-phase streamlines with no slip velocity [38], d) the condensed liquid cannot evaporate. Correspondingly, the fundamental equations are based on the single-fluid Eulerian model employed to predict the compressible supersonic flow and the condensation phenomenon. The governing equations including the mass, momentum and energy equations are used for the gas-liquid mixture. In addition, two transport equations are coupled to model the phase change from the gaseous phase to the liquid phase, namely, the conservation of the liquid mass fraction and droplet number.

2.1 Conservation equations for gas-liquid mixture

The conservation equations of mass, momentum and energy for the vapour-liquid mixture are described as follows.

$$\frac{\partial \rho}{\partial t} + \frac{\partial (\rho u_j)}{\partial x_j} = S_m \tag{1}$$

$$\frac{\partial}{\partial t}\left(\rho u_i\right) + \frac{\partial}{\partial x_j}\left(\rho u_j u_i\right) = -\frac{\partial p}{\partial x_i} + \frac{\partial \tau_{ij}}{\partial x_j} + S_{u_i} \tag{2}$$

$$\frac{\partial}{\partial t}(\rho H) + \frac{\partial}{\partial x_j}(\rho u_j H + p) = -\frac{\partial}{\partial x_j}(\lambda_{eff}\frac{\partial T}{\partial x_j}) + \frac{\partial}{\partial x_j}(u_i \tau_{ij}) + S_h \tag{3}$$

where ρ, u_i, p, T and H are the density, velocity, pressure, temperature and total enthalpy, respectively. λ_{eff} is the effective conductivity, $\lambda_{eff} = \lambda_v + \lambda_t$, where λ_v and λ_t are the vapour conductivity and turbulent thermal conductivity, respectively. The source terms, S_m, S_{u_i} and S_h account for the mass, momentum and energy transfer associated with

condensation.

The fluid flow within the supersonic nozzles is violently turbulent and a suitable turbulence model is needed to capture the complicated compressible flows. For this purpose, the shear stress transport (SST) *k*-*ω* turbulence model is used due to the good accuracy to predict the supersonic nozzle flow [39] and the condensation phenomenon [40]. The equations for these turbulence models are not documented here for brevity, however, they are well documented by Menter [41].

2.2 Liquid phase equations

Two transport equations are utilized to describe the phase change process during the CO_2 condensation in supersonic nozzles. The conservation equations include the liquid fraction (Y) and droplet number (N):

$$\frac{\partial(\rho Y)}{\partial t}+\frac{\partial}{\partial x_j}\left(\rho Y u_j\right)=S_Y \tag{4}$$

$$\frac{\partial(\rho N)}{\partial t}+\frac{\partial}{\partial x_j}\left(\rho N u_j\right)=\rho J \tag{5}$$

where the source term S_Y describes the condensation rate of the water vapour, and J is the nucleation rate, respectively. N is the number of droplets per volume. The source terms are defined as follows:

$$S_m=-\Gamma \tag{6}$$

$$S_{u_i}=-u_i\Gamma \tag{7}$$

$$S_{h_l}=-h\Gamma \tag{8}$$

$$S_Y=\Gamma \tag{9}$$

$$\Gamma=\frac{4\pi r_c^{\,3}}{3}\rho_l J+4\pi r^2\rho_l N\frac{dr}{dt} \tag{10}$$

where Γ is the condensation mass per unit vapour volume per unit time. ρ_l is the droplet density, r is the droplet radius. dr/dt is the growth rate of droplets. The r_c is the Kelvin-Helmholtz critical droplet radius.

The nucleation rate, J, is calculated by the modified classical nucleation theory, which uses the non-isothermal correction of Kantrowitz [42] as follows:

$$J = \frac{q_c}{1+\phi}\frac{\rho_v^{\,2}}{\rho_l}\sqrt{\frac{2\sigma}{\pi m_v^{\,3}}}\exp\left(-\frac{4\pi\sigma}{3k_B T_v}r_c^{\,2}\right) \tag{11}$$

where q_c is the condensation coefficient, σ is the liquid surface tension, m_v is the mass of a vapour molecule, k_B is the Boltzmann's constant, T_v is the vapour temperature. ϕ is a correction factor proposed by Kantrowitz [42]:

$$\phi = 2\frac{\gamma-1}{\gamma+1}\frac{h}{R_v T_v}\left(\frac{h}{R_v T_v}-\frac{1}{2}\right) \tag{12}$$

where γ is the specific heat ratio, R_v is the gas constant.

The critical droplet radius, r_c is defined as:

$$r_c = \frac{2\sigma}{\rho_l R_v T_v \ln(S)} \tag{13}$$

where S is the supersaturation ratio, which is defined as the ratio of vapour pressure, p_v to the equilibrium saturation pressure, $p_{sat}(T)$.

$$S = \frac{p_v}{p_{sat}(T)} \tag{14}$$

The growth rate of droplets due to evaporation and condensation, dr/dt, is calculated by Young's model [43],

$$\frac{dr}{dt} = \frac{\lambda_v\left(T_s - T_v\right)}{\rho_l h r}\frac{\left(1-r^*/r\right)}{\left(\dfrac{1}{1+2\beta\mathrm{Kn}}+3.78(1-\nu)\dfrac{\mathrm{Kn}}{\mathrm{Pr}}\right)} \tag{15}$$

where h is the specific enthalpy, T_s is the saturated temperature, Pr is the Prandtl number, Kn is the Knudsen number, and v is the modelling correction coefficient:

$$v = \frac{RT_s}{h}\left(\alpha - 0.5 - \frac{2-q_c}{2q_c}\left(\frac{\gamma+1}{2\gamma}\right)\left(\frac{c_{pv}T_s}{h}\right)\right) \tag{16}$$

where α and β are the modelling parameters, c_{pv} is the vapour constant pressure specific heat. The modelling parameters used in this study are as follows: q_c = 1.0, α = 1.0, β = 0.0.

2.3 Numerical implementation

The commercial package ANSYS FLUENT 18 is employed as the computational platform. The conservation equations (1) - (3) for vapour-liquid mixture are directly solved in FLUENT, while the governing equations (4) - (16) for liquid phase and the source terms are performed by the User-Defined-Scalar (UDS) and User-Defined-Function (UDF) interfaces. The implicit density-based solver is employed to perform the numerical simulation considering the supersonic and condensing flows. The second-order upwind scheme is adopted for an accurate spatial prediction. The transient state solution is used in the numerical studies with a time step of 10^{-6} s. The pressure inlet conditions are assigned for the nozzle entrance, while the nozzle exit utilises the pressure outlet condition.

3 Results and discussion

3.1 Model validation

The Gyarmathy's high-pressure nozzle [44] is employed to evaluate the CFD modelling of the condensation behaviour in supersonic flows. The high-pressure nozzle is designed as a half-Laval nozzle with the height of the throat of 10.00 mm, as shown

in Fig. 1. The contour of one side of the supersonic nozzle is a flat wall, where the pressure tap is installed to test the static pressure during the experiments. The other side of the supersonic nozzle is a curved wall as described in Table 1. The main dimensions include the length of the converging section of 30 mm and the length of the diverging section of 100 mm. The heights of the inlet and outlet of the supersonic nozzle are 19.99 mm and 17.91 mm, respectively. The computational conditions and modelling parameters are listed in Table 2.

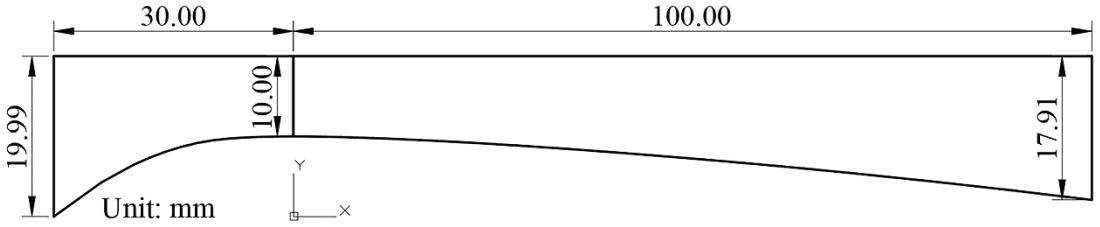

Fig. 1 Geometry of Gyarmathy's nozzle

Table 1. Curve contour of Gyarmathy's nozzle

x (mm)	y (mm)	x (mm)	y (mm)	x (mm)	y (mm)	x (mm)	y (mm)
-30	6.51	-4	16.45	16	16.04	44	14.22
-24	10.79	-2	16.49	18	15.94	50	13.74
-20	12.97	0	16.50	20	15.84	54	13.40
-18	13.85	2	16.49	22	15.73	60	12.87
-16	14.60	4	16.46	24	15.61	64	12.50
-14	15.21	6	16.42	26	15.49	70	11.92
-12	15.69	8	16.36	28	15.37	80	10.89
-10	16.03	10	16.29	30	15.24	90	9.78
-8	16.24	12	16.22	34	14.97	100	8.59
-6	16.37	14	16.13	40	14.53		

Table 2. The computational condition for Gyarmathy's nozzle

Inlet conditions	Outlet conditions	Wall conditions	Modelling parameters
Total pressure: 89 bar Total temperature: 619.96 K	Supersonic flows	No-slip Adiabatic wall	q_c = 1.0, α = 1.0, β = 0.0

The resolution of the grid is one of the key issues for the prediction of the CO_2 condensing behaviour in supersonic flows, which presents an extraordinarily complicated fluid flow phenomenon including the transonic flow, shock wave and flow separation. For this reason, a multi-block structure mesh is performed for the supersonic nozzle, while the fine grid scheme is adopted in the boundary layer to ensure that $y+$ is less than 1 for the SST k-ω turbulence model. The grid of Gyarmathy's nozzle is shown in Fig. 2. The numerical results are performed with a medium mesh of 22800 cells after evaluating the mesh independence with 7920, 22800 and 40000 cells, respectively. Fig. 3 presents the numerical and experimental results of the flow field and droplet radius inside the high-pressure nozzle. The results of the calculated static pressure are in good agreement with the experimental data. The model accurately captures the onset of the condensation process, which occurs approximately at x = 0.033 m. Furthermore, the CFD model predicts the droplet radius of 0.121 μm at x = 0.093 m, while the measurement was approximately 0.143 μm in the experimental test. This indicates that the developed CFD modelling accurately predicts and captures the condensation behaviour in supersonic flows.

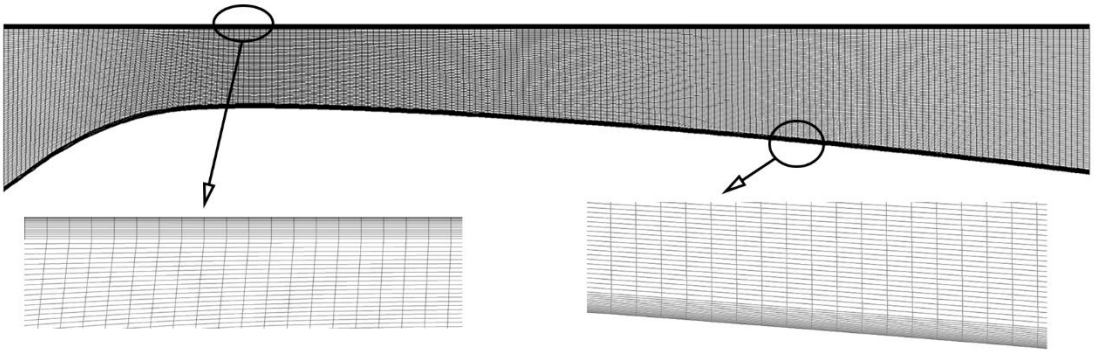

Fig. 2 Grid of Gyarmathy's nozzle

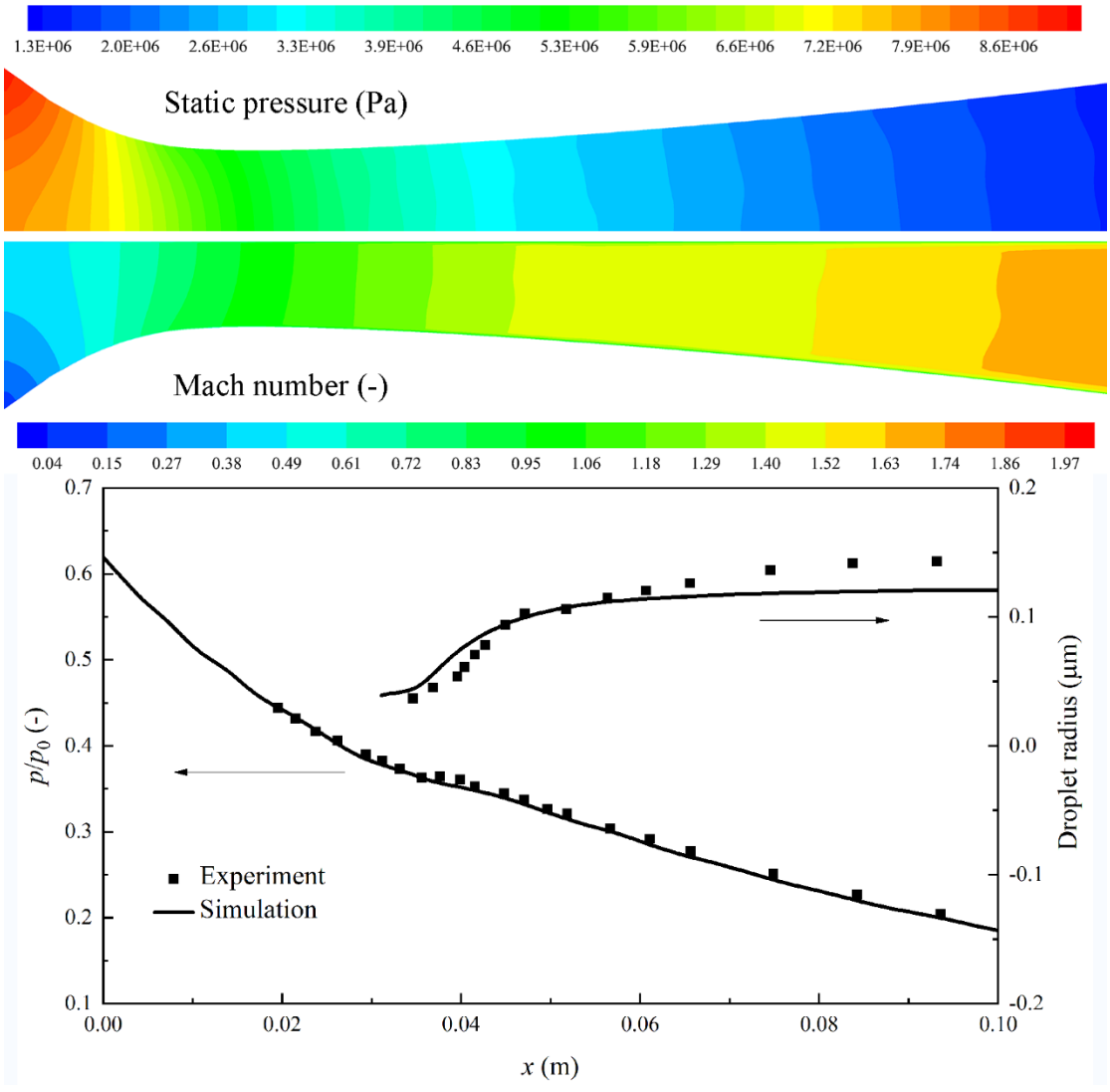

Fig. 3 Numerical and experimental results of flow field and droplet radius inside Gyarmathy's nozzle

3.2 Effect of CO_2 condensation on the flow field

The converging-diverging nozzle from Moses and Stein experiments [45] was employed to study the non-equilibrium condensation of CO_2 in supersonic flows, as shown in Fig. 4. The configuration and main dimensions of the supersonic nozzle used in the CFD simulation are described in Fig. 4 and Table 3, respectively. The area ratio of the supersonic nozzle is 3.55, which is defined as the ratio of the nozzle exit area to the nozzle throat area. The 2D geometry was employed in the CFD model to evaluate the performance of the supersonic nozzle. The computational domain was discretized by a structured mesh to reduce the numerical diffusion, as shown in Fig. 4. Approximately 50 000 cells were employed for the numerical simulation after the mesh independence tests. The computational conditions and modelling parameters are listed in Table 4.

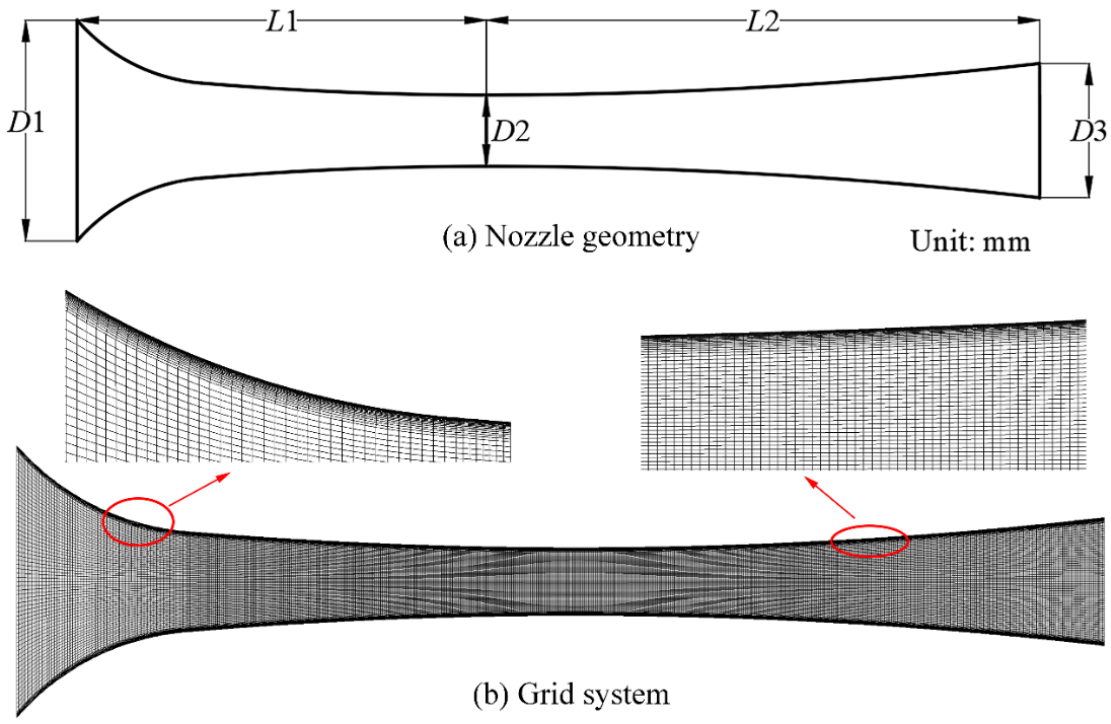

Fig. 4 Geometry and grid of converging-diverging nozzle

Table 3. Dimensions of the converging-diverging nozzle

Geometrical parameters	Value (mm)
Diameter of nozzle inlet ($D1$)	40.00
Diameter of nozzle throat ($D2$)	10.00
Diameter of nozzle outlet ($D3$)	18.85
Converging length of the supersonic nozzle ($L1$)	57.53
Diverging length of the supersonic nozzle ($L2$)	102.47

Table 4. The computational condition for the converging-diverging nozzle

Inlet conditions	Outlet conditions	Wall conditions	Modelling parameters
Total pressure: 40 bar Total temperature: 283 K	Supersonic flows	No-slip, adiabatic wall	$q_c = 1.0$, $\alpha = 1.0$, $\beta = 0.0$

Fig. 5 describes the contours of CO_2 Mach number based on the dry gas and condensing flow models. The results clearly demonstrate the effect of the condensation phenomenon on the CO_2 expansion processes inside the converging-diverging nozzle. It can be seen that the dry gas and condensing flows both achieve the supersonic velocity in the diverging part, while they both predict the choked flows at the nozzle throat. The increase of the Mach number shows that the CO_2 gas flows further accelerate and expand to the nozzle exit. However, the dry gas and condensing flow approaches predict different Mach number values. The dry gas assumption over-predicts a further expansion than the condensing flow model. For example, the dry gas

predicts a Mach number of 2.33 at the exit plane of the supersonic nozzle, while the condensing flow gives a Mach number of 2.18. The difference of Mach number values between these two approaches reaches 6.9% at the nozzle outlet for CO_2 flows. This indicates that the CO_2 condensation significantly influences the expansion characteristics in the supersonic flows.

Fig. 6 shows the Mach number profiles at the central line of the supersonic model for the dry gas and condensing flow models. It is also demonstrated that the dry gas assumption predicts a higher Mach number in the diverging part of the supersonic nozzle than the condensing flow model, which means that the dry gas assumption over-predicts the expansion characteristics of the supersonic flows. This clearly illustrates the significant influence of the condensation phenomenon due to the supersonic flow. From the profile of the condensing flow model, one can see that the CO_2 Mach number increases along the supersonic nozzle and starts to deviate from the dry gas assumption in the diverging part of the supersonic nozzle. This indicates that the occurrence of the condensed liquids causes more energy losses, which cannot be described by the dry gas assumption.

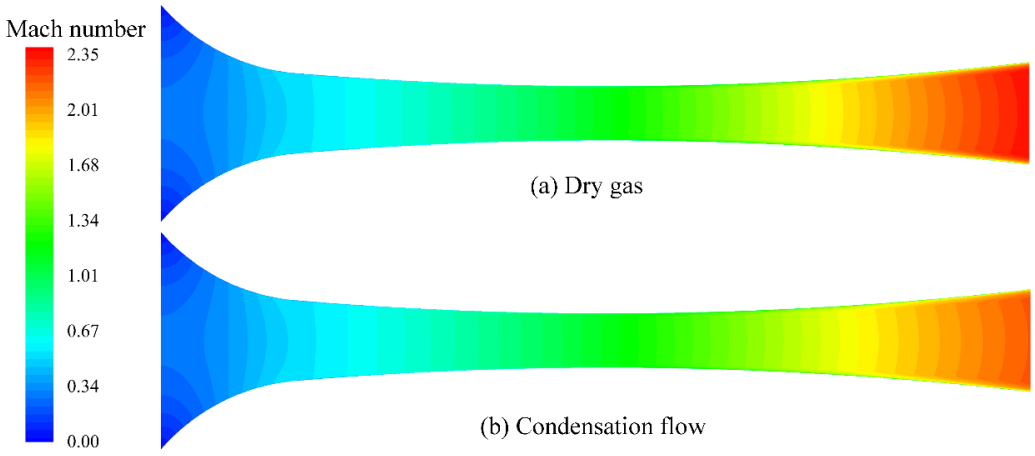

Fig. 5 CO_2 Mach number contours in converging-diverging nozzles

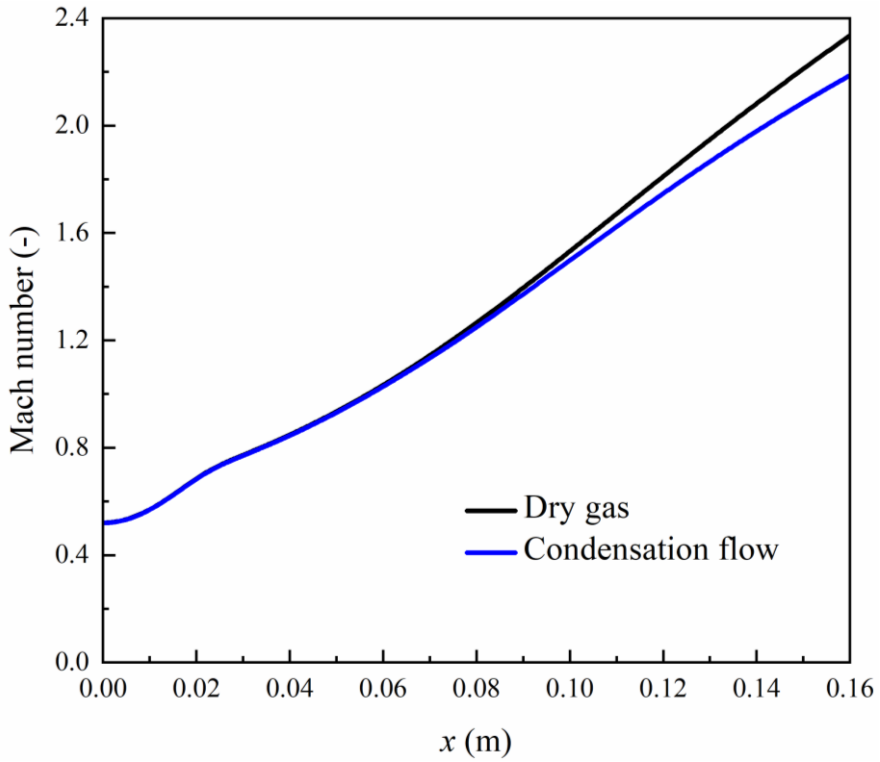

Fig. 6 CO_2 Mach number profiles at the central line of converging-diverging nozzles

Fig. 7 describes the distribution of the static temperature of CO_2 flow along the supersonic nozzle for the dry gas assumption and condensing flow model. The differences are evident between the dry gas and condensing flow simulations. Without considering the condensation process inside the supersonic nozzle, the dry gas assumption obtains unphysical results, i.e., the static temperature limitlessly decreases to the nozzle exit. For instance, the dry gas assumption predicts the minimum static temperature of approximately 177 K, which is much lower than the triple point of 217 K for CO_2. Combining the pressure-temperature profiles in Fig. 8, it correspondingly leads to the confusion that the formation of CO_2 ice may occur in such a low temperature. In fact, this is an artefact due to the assumption of the dry gas model.

For the condensing flow model, the static temperature decreases along the supersonic nozzle and presents a sudden jump when the condensation phenomenon of

CO_2 occurs downstream of the nozzle throat. The heat is released during the phase change from the vapour to the liquid, which forces the vapour-liquid mixture to return to the equilibrium state. The static temperature distribution distinctly shows that the condensing flow model limits the drop of the static temperature lower than the triple point. This thereby eliminates the artefact of the CO_2 ice formation. On the other hand, it also demonstrates that the developed condensing flow model accurately captures the CO_2 condensation process in supersonic flows.

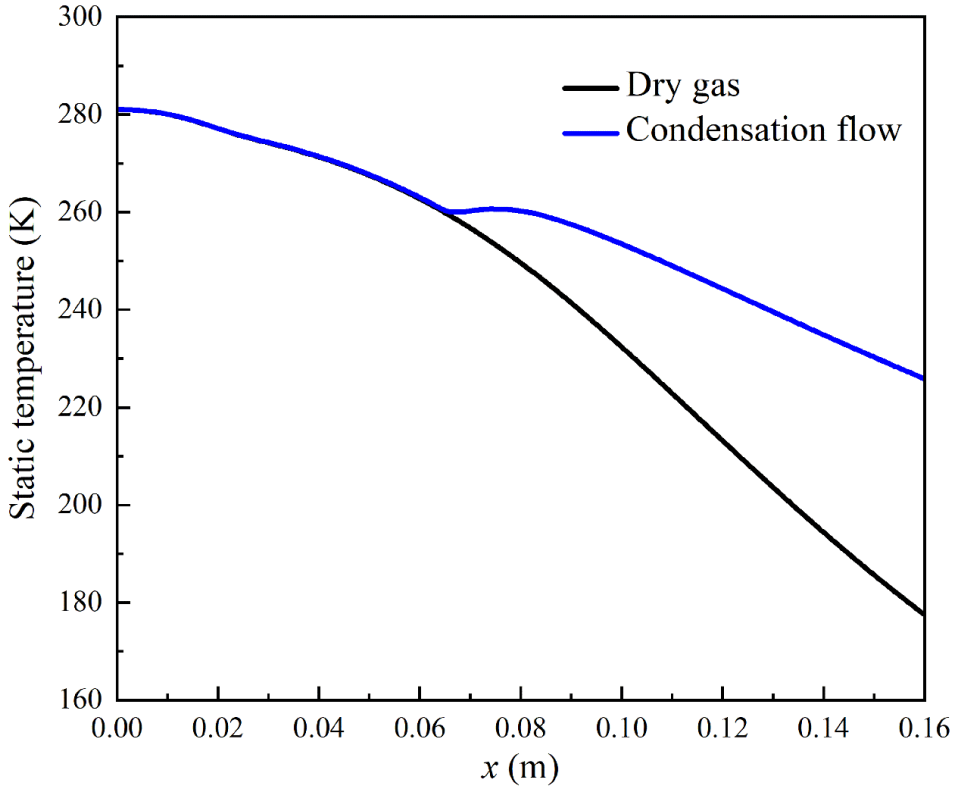

Fig. 7 Static temperature along the converging-diverging nozzle for dry gas and condensing flow models

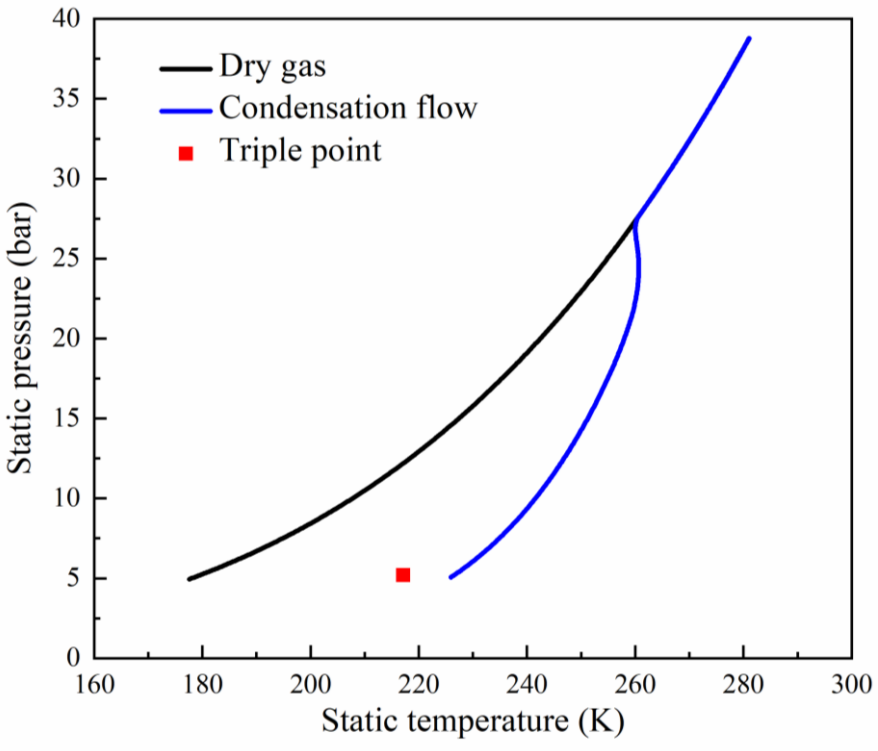

Fig. 8 Pressure-temperature profiles for CO_2 flows

3.3 CO_2 condensation characteristics

Fig. 9 presents the degree of supercooling and the degree of supersaturation for the flow of CO_2 inside the converging-diverging nozzle, which both describe the vapour state during the supersonic expansion. The degree of supercooling, $\Delta T = T_s - T_v$, is defined as the difference between the saturation temperature (T_s) and local vapour temperature (T_v). The nucleation rate profile at the central line of the supersonic nozzle is shown in Fig. 10. One can see that the condensation does not occur immediately when the CO_2 reaches the saturation state at x=0.038 m. The reason is that we only consider the spontaneous condensation of the CO_2 fluids without involving heterogeneous condensation, i.e., the effect of foreign particles present in the flow. The static pressure and temperature sequentially decrease because of the vapour expansion in the diverging part of the supersonic nozzle. The vapour correspondingly diverges

further from the equilibrium state. For instance, the peaks of the degree of supercooling and the degree of supersaturation are approximately 8.36 K and 1.14 at x=0.066 m, respectively. The highly non-equilibrium state induces the appearance of the nucleation and condensation of CO_2 in a remarkably small area, which can be observed in the distribution of the nucleation rate in Fig. 10. The vapour returns to the quasi-equilibrium state due to the latent heat release to the vapour phase during the condensation process, as shown in Fig. 9.

Fig. 11 presents the liquid fraction along the supersonic nozzle. Combined with the distribution of the nucleation rate in Fig. 10, it is observed that the liquid fraction increases with the occurrence of the nucleation process. The rapid nucleation and condensation induce the sharp increase of the liquid fraction until the exit plane of the supersonic nozzle. The liquid fraction reaches a peak value of approximately 0.186 at this point, which shows that the amount of the liquid fraction has a significant influence on the vapour phase. Fig. 12 describes the distribution of the droplet radius along the flow direction in the supersonic nozzle. We can see that the droplet radius presents a similar distribution with the liquid fraction. The maximum size of the condensed CO_2 droplets is approximately 1 μm at the nozzle exit. This indicates that the assumptions of the tiny particles following the vapour phase and the no-slip velocity between the vapour and liquid phases are reasonable in the CFD modelling of the CO_2 condensation phenomenon inside the supersonic nozzle.

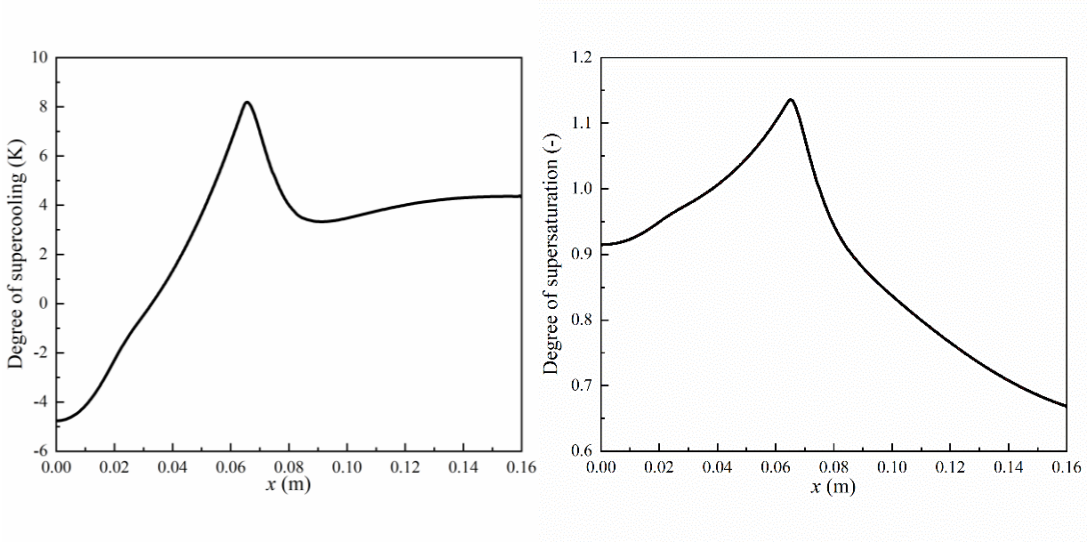

Fig. 9 Degree of supercooling and degree of supersaturation along the converging-diverging nozzle

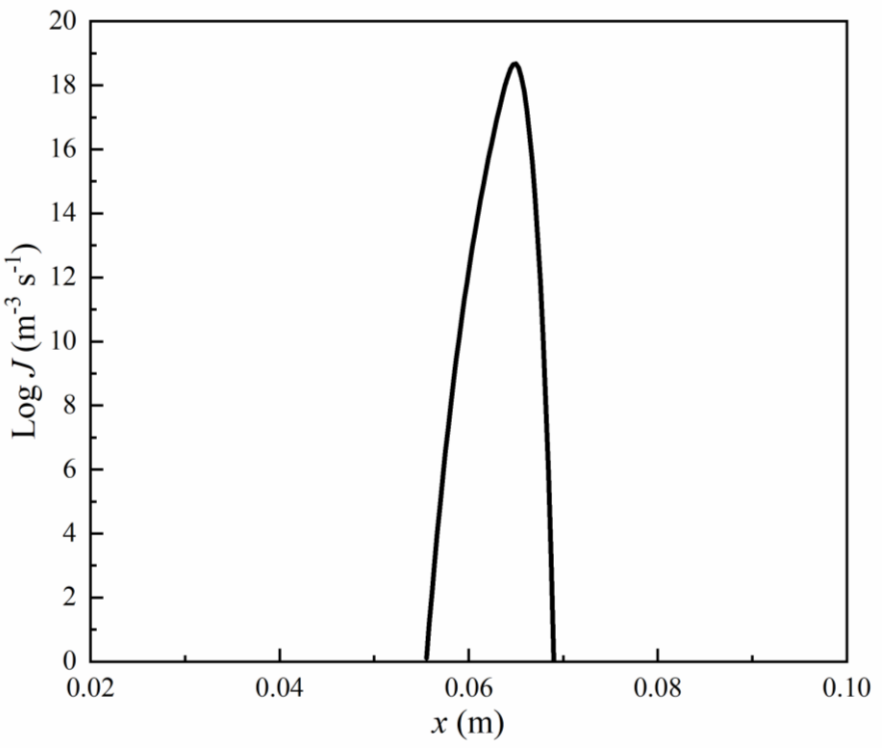

Fig. 10 Nucleation rate along the converging-diverging nozzle

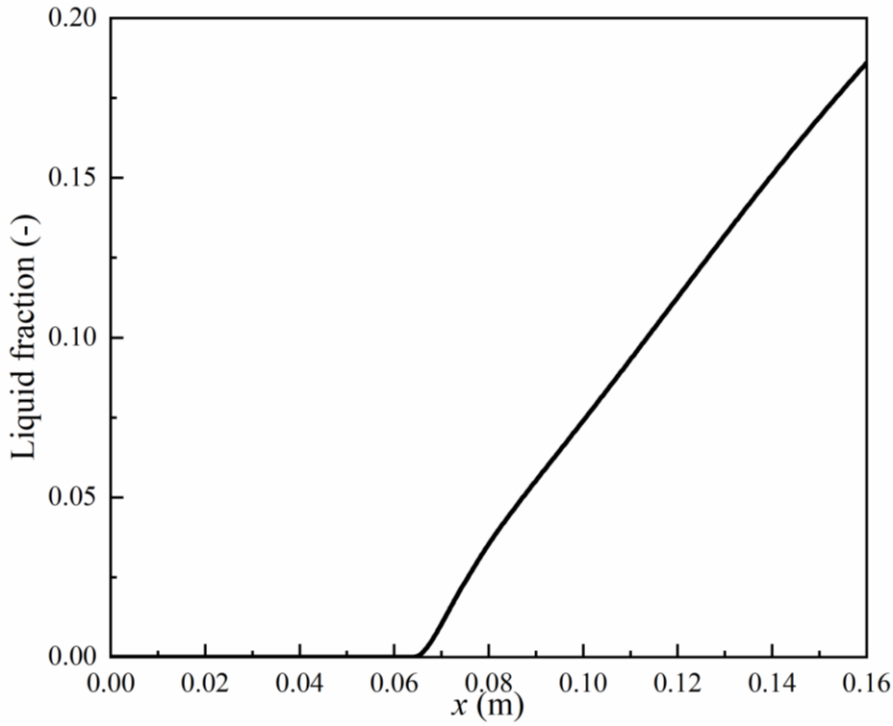

Fig. 11 Liquid fraction along the converging-diverging nozzle

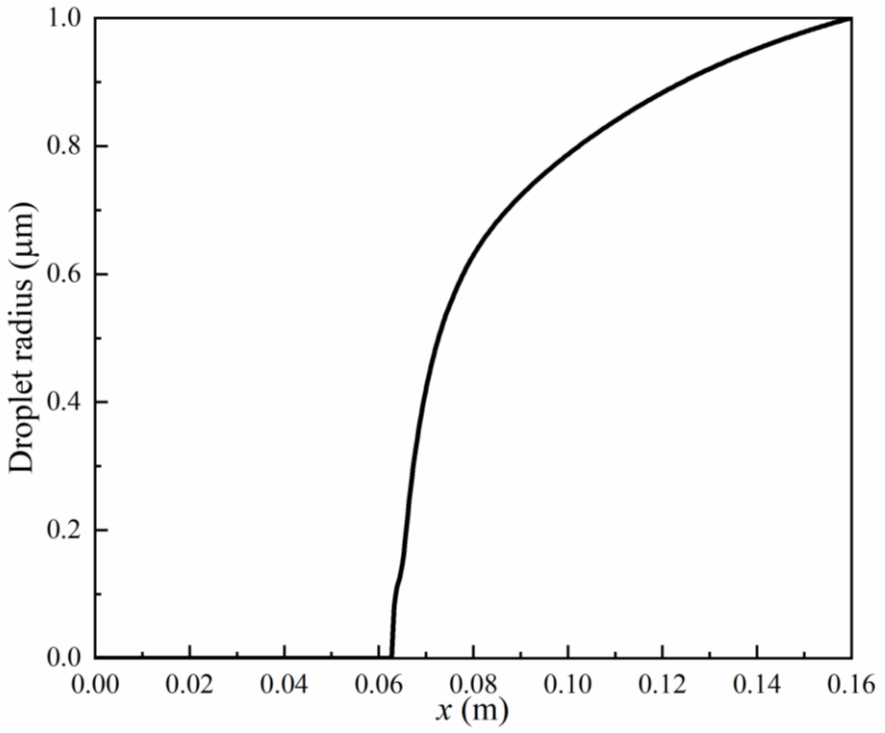

Fig. 12 Droplet radius along the converging-diverging nozzle

3.4 Discussion

This study presents the preliminary results of the CO_2 phase change in supersonic

flows, where only the Laval nozzle is considered without implementation of a swirling device and a diffuser for a supersonic separator. Correspondingly, the flow behaviour is simplified for the numerical simulation, while more complicated flows are neglected including the shock wave, flow separation, strong swirling flows.

Bian et al. [22] carried out the numerical simulation for the water vapour removal inside a supersonic separator, and the single-phase flow model predicted a minimum value of the static temperature of 199.43 K. Hu et al. [26] predicted a static temperature lower than 180 K without considering the phase change processes of the water vapour in a supersonic separator. Moreover, Secchi et al. [22] obtained the minimum static temperature of approximately 140 K according to the 1D model without involving condensing flow processes. Considering our numerical results of the condensing flow behaviour, the assumption of the dry gas model over-predicts the gas expansion in supersonic flows and give an artefact of the static temperature. This also demonstrates that the implementation of the condensing flow model is essential to estimate the possibility of the removal of either water vapour or CO_2 using supersonic separation.

Furthermore, it is worth noting that the condensing flow model is a semi-empirical model, which employs the modelling parameters to predict the nucleation and droplet growth processes. The values of the modelling parameters, α, β, q_c, are various in different investigator' models. Starzmann et al. [46] validated their model against experimental data from the Moses and Stein nozzle [45] with $q_c = 1.0$, $\alpha = 11.0$. Grübel et al. [47] used the modelling parameters $q_c = 1.0$, $\alpha = 0.0$, $\beta = 0.0$ to validate and verify their CFD model with the Moses and Stein nozzle [45]. In this study, the model

validation indicates that the modelling parameters, q_c = 1.0, α = 1.0, β = 0.0 show a good agreement with experimental data from the Gyarmathy's high-pressure nozzle [44] with the working fluid of water vapour. The same modelling parameters are implemented for CO_2 simulation because there are no available experimental data for the validation and verification of CO_2 condensation in supersonic flows. The computational results, at least, demonstrate in the qualitative analysis that it is a potential way to condense CO_2 in supersonic flows. The condensing flow model, therefore, needs to be further validated against experimental tests with the working fluid of CO_2 in future work.

5 Conclusions

This study shows an alternative approach of mitigating CO_2 emissions to the environment. The modelling using computational fluid dynamics developed in this study can predict the nucleation and condensation of CO_2 due to the non-equilibrium phenomenon in supersonic flows. The single-fluid flow model is employed for the modelling with the assumption of no-slip velocity between vapour and liquid phases, while two conservation equations of liquid fraction and liquid number are used to describe the phase change processes.

The developed condensing flow model and conventional dry gas model are compared to show the different predictions on the flow structures and condensation characteristics during the CO_2 phase change in supersonic flows. The dry gas assumption predicts an incorrect distribution of the static temperature without considering the condensation process, which leads to a minimum static temperature of

approximately 177 K, much lower than the CO_2 triple point of 217 K. This may result in the misunderstanding of CO_2 ice formation problem in such a low temperature. The condensing flow model eliminates this artefact by considering the heat and mass transfer during the condensation process in supersonic flows. The condensing flow model predicts the liquid fraction of 18.6% of the total mass due to the high expansion of the supersonic flow. The amount of the condensed liquid influences the vapour phase by heat and mass transfer.

This study has presented an alternative solution of mitigating CO_2 emissions in an efficient and environment-friendly way. The developed CFD model provides a basic method to predict non-equilibrium condensation of CO_2 in supersonic flows. This study provides the insights to design and optimisation of the supersonic separation technique for future applications of CO_2 removal contributing to CCS.

Acknowledgements

The research leading to these results has received funding from the People Programme (Marie Curie Actions) of the European Union's Seventh Framework Programme (FP7/2007-2013) under REA grant agreement no. 609405 (COFUNDPostdocDTU).

References

[1] Yan J, Zhang Z. Carbon Capture, Utilization and Storage (CCUS). Applied Energy. 2019;235:1289-99.

[2] Görke R, Hu W, Dunstan M, Dennis JS, Scott SA. Exploration of the material property space for chemical looping air separation applied to carbon capture and storage.

Applied Energy. 2018;212:478-88.

[3] Roussanaly S, Aasen A, Anantharaman R, Danielsen B, Jakobsen J, Heme-De-Lacotte L, et al. Offshore power generation with carbon capture and storage to decarbonise mainland electricity and offshore oil and gas installations: A techno-economic analysis. Applied Energy. 2019;233:478-94.

[4] Jia B, Tsau J-S, Barati R. A review of the current progress of CO2 injection EOR and carbon storage in shale oil reservoirs. Fuel. 2019;236:404-27.

[5] Kim TH, Cho J, Lee KS. Evaluation of CO2 injection in shale gas reservoirs with multi-component transport and geomechanical effects. Applied Energy. 2017;190:1195-206.

[6] Singh H. Impact of four different CO2 injection schemes on extent of reservoir pressure and saturation. Advances in Geo-Energy Research. 2018;2:305-18.

[7] Zhang L, Ezekiel J, Li D, Pei J, Ren S. Potential assessment of CO2 injection for heat mining and geological storage in geothermal reservoirs of China. Applied Energy. 2014;122:237-46.

[8] Chu F, Yang L, Du X, Yang Y. Mass transfer and energy consumption for CO2 absorption by ammonia solution in bubble column. Applied Energy. 2017;190:1068-80.

[9] Zhao R, Zhao L, Deng S, Song C, He J, Shao Y, et al. A comparative study on CO2 capture performance of vacuum-pressure swing adsorption and pressure-temperature swing adsorption based on carbon pump cycle. Energy. 2017;137:495-509.

[10] Yousef AM, El-Maghlany WM, Eldrainy YA, Attia A. New approach for biogas purification using cryogenic separation and distillation process for CO2 capture.

Energy. 2018;156:328-51.

[11] Medrano J, Potdar I, Melendez J, Spallina V, Pacheco-Tanaka DA, van Sint Annaland M, et al. The membrane-assisted chemical looping reforming concept for efficient H 2 production with inherent CO 2 capture: Experimental demonstration and model validation. Applied Energy. 2018;215:75-86.

[12] Mondal MK, Balsora HK, Varshney P. Progress and trends in CO2 capture/separation technologies: A review. Energy. 2012;46:431-41.

[13] Rezakazemi M, Darabi M, Soroush E, Mesbah M. CO2 absorption enhancement by water-based nanofluids of CNT and SiO2 using hollow-fiber membrane contactor. Separation and Purification Technology. 2019;210:920-6.

[14] Nabipour M, Keshavarz P, Raeissi S. Experimental investigation on CO2 absorption in Sulfinol-M based Fe3O4 and MWCNT nanofluids. International Journal of Refrigeration. 2017;73:1-10.

[15] Kim JH, Jung CW, Kang YT. Mass transfer enhancement during CO2 absorption process in methanol/Al2O3 nanofluids. International Journal of Heat and Mass Transfer. 2014;76:484-91.

[16] Zhang Z, Cai J, Chen F, Li H, Zhang W, Qi W. Progress in enhancement of CO2 absorption by nanofluids: A mini review of mechanisms and current status. Renewable Energy. 2018;118:527-35.

[17] Yang Y, Walther JH, Yan Y, Wen C. CFD modeling of condensation process of water vapor in supersonic flows. Applied Thermal Engineering. 2017;115:1357-62.

[18] Wen C, Yang Y, Walther JH, Pang KM, Feng Y. Effect of delta wing on the

particle flow in a novel gas supersonic separator. Powder Technology. 2016;304:261-7.

[19] Yang Y, Wen C, Wang S, Feng Y. Theoretical and numerical analysis on pressure recovery of supersonic separators for natural gas dehydration. Applied Energy. 2014;132:248-53.

[20] Yang Y, Li A, Wen C. Optimization of static vanes in a supersonic separator for gas purification. Fuel Processing Technology. 2017;156:265-70.

[21] Yang Y, Wen C. CFD modeling of particle behavior in supersonic flows with strong swirls for gas separation. Separation and Purification Technology. 2017;174:22-8.

[22] Secchi R, Innocenti G, Fiaschi D. Supersonic Swirling Separator for natural gas heavy fractions extraction: 1D model with real gas EOS for preliminary design. Journal of Natural Gas Science and Engineering. 2016;34:197-215.

[23] Bian J, Jiang W, Teng L, Liu Y, Wang S, Deng Z. Structure improvements and numerical simulation of supersonic separators. Chemical Engineering and Processing: Process Intensification. 2016;110:214-9.

[24] Wang Y, Hu D. Experimental and numerical investigation on the blade angle of axial-flow swirling generator and drainage structure for supersonic separators with diversion cone. Chemical Engineering Research and Design. 2018;133:155-67.

[25] Wang Y, Hu D. Structure improvements and numerical simulation of supersonic separators with diversion cone for separation and purification. RSC Advances. 2018;8:10228-36.

[26] Hu D, Wang Y, Ma C. Numerical simulation of supersonic separator with

axial or tangential outlet in reflow channel. Chemical Engineering and Processing: Process Intensification. 2018;124:109-21.

[27] Niknam PH, Mortaheb H, Mokhtarani B. Effects of fluid type and pressure order on performance of convergent–divergent nozzles: An efficiency model for supersonic separation. Asia-Pacific Journal of Chemical Engineering. 2018;13:e2181.

[28] Liu X, Liu Z. Numerical investigation and improvement strategy of flow characteristics inside supersonic separator. Separation Science and Technology. 2018;53:940-52.

[29] Jiang W, Bian J, Wu A, Gao S, Yin P, Hou D. Investigation of supersonic separation mechanism of CO2 in natural gas applying the Discrete Particle Method. Chemical Engineering and Processing - Process Intensification. 2018;123:272-9.

[30] Ma Q-F, Hu D-P, Jiang J-Z, Qiu Z-H. A turbulent Eulerian multi-fluid model for homogeneous nucleation of water vapour in transonic flow. International Journal of Computational Fluid Dynamics. 2009;23:221-31.

[31] Ma Q-F, Hu D-P, Jiang J-Z, Qiu Z-H. Numerical study of the spontaneous nucleation of self-rotational moist gas in a converging–diverging nozzle. International Journal of Computational Fluid Dynamics. 2010;24:29-36.

[32] Shooshtari SR, Shahsavand A. Reliable prediction of condensation rates for purification of natural gas via supersonic separators. Separation and Purification Technology. 2013;116:458-70.

[33] Shooshtari SHR, Shahsavand A. Predictions of wet natural gases condensation rates via multi-component and multi-phase simulation of supersonic

separators. Korean Journal of Chemical Engineering. 2014;31:1845-58.

[34] Castier M. Modeling and simulation of supersonic gas separations. Journal of Natural Gas Science and Engineering. 2014;18:304-11.

[35] Shooshtari SR, Shahsavand A. Optimal operation of refrigeration oriented supersonic separators for natural gas dehydration via heterogeneous condensation. Applied Thermal Engineering. 2018;139:76-86.

[36] Kim I, Peroomian O, Yang X. Modeling of spontaneous condensation in high-speed expansion of gaseous mixture. International Journal of Heat and Mass Transfer. 2015;86:710-20.

[37] Abadi SNR, Ahmadpour A, Abadi S, Meyer JP. CFD-based shape optimization of steam turbine blade cascade in transonic two phase flows. Applied Thermal Engineering. 2017;112:1575-89.

[38] Dykas S, Majkut M, Smołka K, Strozik M. Study of the wet steam flow in the blade tip rotor linear blade cascade. International Journal of Heat and Mass Transfer. 2018;120:9-17.

[39] Dykas S, Wróblewski W. Numerical modelling of steam condensing flow in low and high-pressure nozzles. International Journal of Heat and Mass Transfer. 2012;55:6191-9.

[40] Ariafar K, Buttsworth D, Al-Doori G, Malpress R. Effect of mixing on the performance of wet steam ejectors. Energy. 2015;93:2030-41.

[41] Menter FR. Two-equation eddy-viscosity turbulence models for engineering applications. AIAA journal. 1994;32:1598-605.

[42] Kantrowitz A. Nucleation in very rapid vapor expansions. The Journal of chemical physics. 1951;19:1097-100.

[43] Young J. The spontaneous condensation of steam in supersonic nozzle. Physico Chemical Hydrodynamics. 1982;3:57-82.

[44] Gyarmathy G. Nucleation of steam in high-pressure nozzle experiments. Proceedings of the Institution of Mechanical Engineers, Part A: Journal of Power and Energy. 2005;219:511-21.

[45] Moses CA, Stein GD. On the growth of steam droplets formed in a Laval nozzle using both static pressure and light scattering measurements. Journal of Fluids Engineering. 1978;100:311-22.

[46] Starzmann J, Hughes FR, White AJ, Grübel M, Vogt DM. Numerical Investigation of Boundary Layers in Wet Steam Nozzles. Journal of Engineering for Gas Turbines and Power. 2016;139:012606-1--8.

[47] Grübel M, Starzmann J, Schatz M, Eberle T, Vogt D, Sieverding F. Two-Phase Flow Modeling and Measurements in Low-Pressure Turbines—Part I: Numerical Validation of Wet Steam Models and Turbine Modeling. Journal of Engineering for Gas Turbines and Power. 2015;137:042602, 1-11.